Effects of large-scale atmospheric circulation on the Baltic Sea wave climate: application of EOF method on multi-mission satellite altimetry data

Fatemeh Najafzadeh
Tallinna Tehnikaulikool
Nadezhda Kudryavtseva (nadezhda.kudryavtseva@taltech.ee)
Tallinna Tehnikaulikool https://orcid.org/0000-0002-1372-0942
Tarmo Soomere
Tallinna Tehnikaulikool

Research Article

Keywords: Baltic Sea, wave climate, satellite altimetry, teleconnections, wave heights, empirical orthogonal functions

Posted Date: March 13th, 2021

DOI: https://doi.org/10.21203/rs.3.rs-284450/v1

Version of Record: A version of this preprint was published at Climate Dynamics on July 29th, 2021. See the published version at https://doi.org/10.1007/s00382-021-05874-x.

Abstract

Wave heights in the Baltic Sea in 1992–2015 have predominantly increased in the sea's western parts. The linear trends in the winter wave heights exhibit a prominent meridional pattern. Using the technique of Empirical Orthogonal Functions (EOF) applied to the multi-mission satellite altimetry data, we link a large part of this increase in the wave heights with the climatic indices of the Scandinavian mode, North Atlantic Oscillation, and Arctic Oscillation. The winter trends show a statistically significant negative correlation (correlation coefficient –0.47±0.19) with the Scandinavian pattern and a positive correlation with the North Atlantic Oscillation (0.31±0.22) and Arctic Oscillation (0.42±0.20). The meridional pattern is associated with more predominant north-westerly and westerly winds driven by the Scandinavian and North Atlantic Oscillation, respectively. All three climatic indices show a statistically significant time-variable correlation with Baltic Sea wave climate during the winter season. When the Scandinavian pattern's influence is strong, North Atlantic and Arctic Oscillations' effect is low and vice versa. The results are backed up by simulations using synthetic data that demonstrate that the percentage of variance retrieved using EOF analysis from the satellite-derived wave measurements is directly related to the percentage of noise in the data and the retrieved spatial patterns are insensitive to the level of noise.

1. Introduction

The knowledge of both long-term changes and short-term variations in the wave climate has great importance for the safety of navigation (e.g., Barbariol et al. 2019), design purposes (e.g., Hemer et al. 2013), coastal protection (e.g., Weisse et al. 2012), and sediment transport (e.g., Masselink et al. 2016). In semi-sheltered seas, such as the Baltic Sea (Fig. 1), due to the limited size of the water body, small changes in the wind direction can lead to large spatiotemporal variations in the wave climate (e.g., Jönsson, Broman and Rahm 2002; Soomere and Räämet 2011; Kudryavtseva and Soomere 2017) and alongshore transport patterns (Soomere et al. 2015). Therefore, to minimise the coastal menaces, economic losses, provide adequate information for engineering and coastal planning in the future, it is crucial to determine the spatial and temporal variability of the wave climate in such regions.

Wave properties in different locations of the Baltic Sea vary significantly over the decades (Soomere and Räämet 2014; Suursaar and Kullas 2009; Różyński 2010). For example, wave intensity showed a quick drop in the northern part of the Baltic proper at the beginning of 1980s, while it had a small increase along the Lithuanian coast (Kelpšaite, Herrmann and Soomere 2008). The average significant wave height (SWH) in this basin, estimated using satellite altimetry was in the range of 0.44–1.94 m during 1991–2015 with an increasing trend of 0.005 m/yr (Kudryavtseva and Soomere 2017). The largest mean wave height of 1.2 m occurs in the Baltic proper (Nikolkina, Soomere, and Räämet 2014; Björkqvist et al., 2018) and also in the Sea of Bothnia even though the seasonal appearance of ice in the Baltic Sea affects the wave growth in this subbasin (Fig. 1). As expected, semi-enclosed areas of this basin, such as the Gulf of Finland, the Gulf of Riga, and the Bay of Bothnia are characterised by a lower range of the mean wave height of 0.5–1.0 m (Tuomi, Kahma and Pettersson 2011; Nikolkina, Soomere and Räämet 2014; Kudryavtseva and Soomere 2017).

The wave heights and periods can reach ~8 m and 10–12 s respectively, in the northern part of the Baltic proper (Tuomi, Kahma and Pettersson 2011) and in the Sea of Bothnia (Björkqvist et al., 2020), ~6 m and 8–11 s at the entrance to the Gulf of Finland, and ~4 m and 6–8 s in the eastern part of this gulf (Räämet, Soomere and Zaitseva-Pärnaste 2010). Most of the wave events with SWH more than 7 m occurred from November to January (Björkqvist et al. 2018), and the roughest wave storms were the prominent ones in November 1969 and January 2005 (Suursaar and Kullas 2009). During the wave storm in January 2005, the measured SWH reached 7.2 m in the northern Baltic proper and 4.5 m in the Gulf of Finland (Soomere et al. 2008).

One of the main drivers of wind direction is the different phases of atmospheric circulation which can be explained in connection with climate change (Wang, Zwiers, and Swail 2004). The Baltic Sea is located in a transition area between the North Atlantic Ocean and the continental area of Eurasia. Consequently, the wave climate in this basin is highly influenced by the North Atlantic Oscillation (NAO), Arctic Oscillation (AO), and Scandinavia pattern (SCAND; previously Eurasia-1; Barnston and Livezey 1987) climate indices.

The NAO pattern is one of the most prominent teleconnection patterns over the North Atlantic and European regions in all seasons (e.g., Walker and Bliss 1932). However, it has the strongest influence over the Baltic Sea in winter (Rózyński 2010) explaining an essential part of wave height variability from December to February. This climatic index consists of the north-south dipole of anomalies with one centre located over Greenland and another in the North Atlantic at latitudes ~40°N. In terms of the wind direction, the positive phase of the NAO corresponds to stronger westerly winds. During the negative phase, westerly winds are weaker, and the winds from the east and north-east are more frequent (Fig. 1; e.g., Trigo, Osborn and Corte-Real 2002).

The AO mode corresponds to the air circulating counterclockwise at ~55°N latitude, in the Arctic. The AO is strongly related to the NAO. When the AO is in its positive phase, a belt of strong winds circulating the North Pole confines colder air inside the Polar Regions (e.g., Thompson and Wallace 1998). In the AO's negative phase, this belt becomes weaker, resulting in a southward movement of colder arctic air into the mid-latitudes, accompanied by increased storminess (Fig. 1). The positive phase of the AO, similarly to the analogous phase of the NAO, corresponds to strong westerly winds over the Baltic Sea region. The negative phase of the AO results in a shift of storm tracks to the south and the winds from the east are more frequent in the region. The NAO and AO are widely used to connect the regional climate variability to the sea level (Andersson, 2002, Jevrejeva et al., 2005), storm events (Surkova, Arkhipkin, and Kislov 2015), SWH (Rózyński 2010), and ice condition (Jevrejeva, Moore, and Grinsted 2003) in the Baltic Sea.

The processes driven by the NAO and AO have a time variable effect on the Baltic Sea region. A significant change in the frequency of cyclonic circulation occurred at the end of the 19th century, which presumably coincided with a retreat of the Little Ice Age (e.g., Omstedt et al. 2004). The water level records showed a changing effect of the NAO and AO on the Baltic Sea sea-level with a decrease in the correlation of the relevant time series with these indices in 1900–1954 (Andersson 2002; Jevrejeva et al. 2005), and an increase in 1980–2000 (Wakelin et al. 2003; Jevrejeva et al. 2005; Suursaar and Sooäär

2007). There are also indications of spatial dependence of the correlation between the NAO index and sea-level. The reported correlations were very low in 1961–1980 at Narva and Pärnu tide gauges (Suursaar and Sooäär 2007) but much stronger at Wismar, Kronstadt, and Cuxhaven during the same time (Jevrejeva et al. 2005). The time variability of the correlation with the NAO index is also prominent in the temperature (e.g., Jacobeit et al. 2001) and ice conditions (e.g., Jevrejeva, Moore and Grinsted 2003). However, the possibility of a time variable effect of the NAO and AO or the other climatic indices on the Baltic Sea wave climate is currently not studied.

The SCAND pattern consists of a main circulation centre over Scandinavia, with weaker centres of an opposite sign over eastern Russia and Western Europe. This pattern affects regional weather conditions and westerlies mostly in winter (Gao, Yu, and Paek 2017). During the negative phase of the SCAND, the wind rotates anticlockwise around the midpoint of the anomaly, creating strong westerly or north-westerly winds over the northern Europe, Scandinavia, and the Baltic Sea region. During the SCAND positive phase, the wind reverses its direction, rotating clockwise, which results in a strong easterly and south-easterly winds belt (Bueh and Nakamura 2007; Gao, Yu and Paek 2017). Fig. 1 shows wind directions during the positive and negative phases of the SCAND over the Baltic Sea (Bueh and Nakamura 2007). This pattern's positive phase blocks the cold air in central Eurasia with below-average temperatures across central Russia and Western Europe.

The most influential atmospheric teleconnections in the Baltic Sea region are NAO, AO, and SCAND. In some studies, the East-Atlantic West-Russia (EAWR), the East Atlantic (EA), the Polar-Eurasia (POL), and the Atlantic Multidecadal Oscillation (AMO) are considered as the drivers of precipitation pattern (Jaagus 2009; Irannezhad, Marttila, and Kløve 2014) and coastal upwelling (Bednorz et al. 2019). However, it is still unclear what are the links between these climatic indices and the wave climate.

There are three different data collecting methods for wave climate studies: modelling, direct measurements and remote sensing. The most common wave models used in the Baltic Sea are the third-generation models WAM (Cavaleri 1997; Hasselmann et al. 1988) and SWAN (Booij, Ris, and Holthuijsen 1999). Based on these models, several hindcasts of the wave climate (Soomere 2005; Cieślikiewicz and Paplińska-Swerpel 2008; Björkqvist et al., 2018; Tuomi et al. 2019) and studies of the annual and decadal changes of wave heights in the Baltic Sea (Soomere and Räämet 2014) were performed. Due to different model parameters and, in particular, depending on the wind forcing, there are mismatches between different model outputs (Tuomi, Kahma, and Pettersson 2011; Soomere and Räämet 2011). Direct measurements are the primary source in the assessment of the local wave climate. However, the relevant devices do not cover the whole area of interest, and the wave measurements are limited to the ice-free time (Tuomi, Kahma, and Pettersson 2011; Madsen, Høyer, and Tscherning 2007; Cieślikiewicz and Paplińska-Swerpel 2008). Hence, direct measurements are restricted only to a few locations and provide a limited knowledge of wave fields' spatial variability.

Significant advances in satellite technology made it possible to obtain homogeneous and continuous wave data over the sea's vast areas. Wave heights derived from high-resolution satellite-based techniques

such as Synthetic Aperture Radar (SAR) in 2012–2017 were compared with in situ data over the Baltic Sea (Rikka et al. 2017). Although there is a good agreement between the SAR and in situ wave height data, the SAR data cover only a short period of 5 years and cannot be used to reconstruct long-term wave climate variability. Satellite altimetry becomes a powerful tool for studying the global scales' wave climate and its relation to the climatic indices (Hannachi 2004). For example, a strong relationship between the interannual variability of SWH (including trends) and both the AO and NAO reveal a connection between these climate patterns and the interannual extreme wave climate in the North Atlantic (Izaguirre et al. 2011)).

However, the use of satellite altimetry is problematic in coastal areas (e.g., Madsen, Høyer, and Tscherning 2007) and partially ice-covered (e.g., Brenner et al. 1983) water bodies like the Baltic Sea. For these reasons, the wave height data from satellites has been used scarcely in this region until recently. A significant effort towards validating the long-term multi-mission wave height data with the available in situ wave measurements in the Baltic Sea region was performed by Kudryavtseva and Soomere (2016). This validation made it possible to study in detail spatial and temporal variations of the Baltic Sea wave climate during the last decades. Significant spatial variability is detected over this basin, which can be explained by a rotation of preferential wind directions rather than an increase in the wind speed (Kudryavtseva and Soomere 2017). However, more effort is needed to identify the main drivers behind the spatial variability of wave heights in the Baltic Sea.

To examine this question in detail, the EOF method (Hannachi 2004) is applied in this study to the wave properties retrieved from satellite altimetry. The EOFs produce an expansion of data in a series of functions that separate the spatiotemporal variations (Niroomandi et al. 2018) and facilitate variability analysis in this domain. The EOF method is a robust tool to determine correlations between the wave climate and climatic indices. It has been widely used to study major modes of climate variability such as the NAO and the El Nino indices (Lionello and Sanna 2005; Nezlin and McWilliams 2003) and to estimate monthly distributions of large-scale sea-level variability on the global scale (Church et al. 2004). The EOF analysis extracted the predominant spatial patterns of monthly averaged wave height variability in wintertime in the northern hemisphere (Shimura, Mori and Mase 2013) and determined the "climate" of seasonal directional wave energy flux in the southern hemisphere (Hemer, Church and Hunter 2010).

Several recent studies have addressed the options for its use in different regions. For example, EOFs helped establish an annual cycle and validate the Mediterranean Sea's spatial wave distribution (Lionello and Sanna 2005; Cañellas et al. 2010; Sartini, Besio and Cassola 2017) and to represent interseasonal variations in the Bengal region (Patra and Bhaskaran 2016). It has also been used to define long-term trends and spatiotemporal variability of wave heights in the Chesapeake Bay (Niroomandi et al. 2018). In the Baltic Sea, this method was applied to the daily maximum values of the total SWH and corresponding windsea and swell heights by using a 5-year hindcast dataset from 1988 to 1993 (Mietus and von Storch 1997). The first EOF of the wave properties revealed a significant anomaly of wave heights in the eastern part of the Baltic Sea. The second and the third EOFs described an anomaly of wave heights from the

southwest to the northeast and an oscillation between the eastern and western parts of the basin, respectively (Mietus and von Storch 1997).

In this study, multi-mission satellite altimetry SWH dataset is used, which was previously validated against all available in situ wave measurements for the Baltic Sea basin (Kudryavtseva and Soomere 2016). Based on these data, spatial and temporal variations of monthly averages of the SWH in the Baltic Sea are analysed by applying the EOF method, and a correlation analysis is performed between the EOF modes and various climatic indices.

The manuscript is described as follows. First, a description of the data and the methodology is introduced in Section 2. In Section 3, the EOF technique is used to retrieve the SWH pattern in the Baltic Sea. Discussion and conclusions are presented Section 4.

2. Materials And Methods

2.1 Satellite altimetry data

The satellite altimetry SWH data from nine satellite missions, namely GEOSAT, ERS-1, TOPEX, ERS-2, ENVISAT, JASON-1, JASON-2, CRYOSAT-2, and SARAL, covering the period from 1992 to 2015 (24 years) with 710344 measurements in total were used in this study. The data have been obtained from the Radar Altimeter Dataset System (RADS) database (Scharroo 2012; Scharroo et al. 2013) and are available for download at http://rads.tudelft.nl/rads/rads.shtml.

Several features of the Baltic Sea such as the presence of ice (Tuomi, Kahma and Pettersson 2011), complicated geometry and the presence of extensive archipelago areas in this relatively small basin (Madsen, Høyer and Tscherning 2007) can significantly affect the quality of satellite data (Kudryavtseva and Soomere 2016). Therefore, data with backscatter coefficient >13.5 cdb, large errors in SWH normalised standard deviation, data closer than 0.2° to the coast, and measured over the sea areas with more than 30% ice concentration were eliminated from further analysis and all measurements were corrected for biases (Kudryavtseva and Soomere 2016). Finally, the data were thoroughly checked for consistency and possible erroneous measurements and validated against the records of in situ data (Kudryavtseva and Soomere 2016).

The resulting dataset (Fig. 2) showed very good quality and is well suitable for the analysis of the Baltic Sea wave climate (Kudryavtseva and Soomere 2017). More than two decades of satellite altimetry data with a large number of measurements provide excellent spatial and temporal coverage over the Baltic Sea. The wave data exhibits intricate variability patterns in both temporal and spatial domain (e.g., Jönsson, Broman and Rahm 2002; Soomere and Räämet 2011; Kudryavtseva and Soomere 2017). To extract these patterns, an EOF analysis (Mietus and von Storch 1997), which separates individual modes of variability, was performed on monthly-averaged SWHs. The analysis was implemented by using the software package "spacetime" (version 1.2-1) in R (version 3.4.4).

2.2 Data gridding

Each satellite altimetry mission measures continuous data only along a specific line. Merging the measurements from different missions into a combined dataset provides much better spatial and temporal coverage but can be prone to gaps. Due to differences in orbits of various missions, the gaps are not regular, which significantly complicates further analysis.

A monthly averaged dataset with a regular rectangular grid was created. The latitudes and longitudes ranged from 54.11°N to 65.57°N and from 10°E to 28.83°E, respectively. Different grid sizes and their effect on the results were thoroughly tested, and the cell size of 0.8°´0.8° showed the optimal performance. Additionally, the grid size effect on the percentage of temporal variability retrieved by EOF was studied. It did not show any dependency on the grid resolution. Despite an increase in resolution, no significant change in the magnitude of reconstructed temporal variability was found.

Due to the nature of the satellite altimetry data, each grid cell has a different number of measurements (Fig. 2). A small number of observations in a particular cell can lead to errors in the EOF results. Hence, the cells with less than a certain number of measurements should be omitted from the analysis. To test the optimal lower cut-off value, the distribution of the number of measurements per grid cell was examined. Interestingly, it is very close to a uniform distribution. To calculate the minimum number of measurements in a single grid cell that does not cause errors in the EOF results, the cut-off values varied in the range of 2%-iles – 5%iles and the EOF analysis results were compared. This test was performed for the whole dataset and several subsets containing measurements during various seasons. The 2nd percentile cut-off provided consistent results and was used in further analysis. As a result, the grid cells that have less than 645 (whole dataset), 181 (winter), 141 (spring), 145 (summer), and 180 (fall) measurements are omitted, leaving more than 99.1% of the data available for the analysis. Most of the omitted data were excluded from the Gulf of Finland, a narrow gulf with a rigged coastline. The spatial distribution of the other omitted data points appeared to be random and, therefore, does not affect the retrieved wave climate spatial patterns.

2.3 Averaging errors

To create a more complete dataset, a monthly average wave height was calculated for each grid cell before applying the EOF method. Due to the natural variability of wave heights on timescales shorter than a month, each monthly average has an uncertainty. This uncertainty σ is estimated as an error of the mean:

$$\sigma = \frac{sd(\mathrm{SWH}_i)}{\sqrt{N}}, \qquad (1)$$

where SWH_i is a set of SWH measured for one month in one grid cell, and N is the number of the data points in each grid cell for that month. A characteristic error of the mean for the whole dataset is estimated as a median of σ. The typical error of the mean in the dataset of interest is ~9%.

2.4 Simulated data sets

To characterise the effect of spatial and temporal gaps (that are inherent in the satellite altimetry data) on the resulting EOFs, simulated data are created and thoroughly tested. The gaps in the data appear due to the variable ice cover, proximity to the coast and satellite tracks. Synthetic data with distinct zonal and meridional patterns are generated and classified as:

Scenario A: A simulated dataset with a distinct zonal (north-south) variation of wave heights, where the wave heights in the northern part (to the north of 59°N) follow a linear trend of 0.005 m/yr and the SWH in the southern part have no distinct long-term variability (Fig. 3). The northern part includes the Bothnian Bay, the Bothnian Sea and the Gulf of Finland and the southern part comprises the Gotland Basin, the Gulf of Riga, the Bornholm Basin and the Arkona Basin.

Scenario B: A simulated dataset with a prominent meridional (west-east) variation of wave heights. The SWH in the western part (to the west of 19.4°E) follow a linear trend of 0.005 m/yr, and in the eastern part, the wave heights have no long-term variability (Fig. 4). The eastern part covers the Bothnian Bay, eastern Bothnian Sea, the Gulf of Finland, the Gulf of Riga and the Eastern Gotland Basin.

These created datasets emulated precisely the same timings and locations as the real multi-mission satellite measurements. The trend of 0.005 m/yr was assigned as a measured wave height trend in the Baltic Sea (Kudryavtseva and Soomere 2017). Gaussian random noise was added to all the simulated data using a Gaussian distribution of a particular width. To test the effect of noise level on the retrieval of the wave height spatial distribution, the Gaussian noise distribution width was varied from 5% to 30% of the total average of the simulated wave heights.

The EOF analysis results on the simulated data are shown in Fig. 3 for the zonal and Fig. 4 for the meridional spatial patterns. The first EOF pattern between northern and southern parts as well as eastern and western parts of the Baltic Sea is visible when the noise level is less than 30%. However, at the noise level higher than 30%, the spatial pattern disappears. These features indicate that (i) spatial and temporal gaps of the satellite altimetry data do not significantly affect the EOF results and (ii) the results of the EOF analysis are susceptible to the noise level.

The percentage of retrieved variance explained by the first EOF mode diminishes with an increase in the noise level (Fig. 5). The low level of introduced noise (5%) results in high variance of ~90% for the simulated datasets in both spatial patterns. However, the highest level of introduced uncertainty (30%) leads to only 18% and 29% of retrieved temporal variabilities for zonal and meridional patterns, respectively. Therefore, this indicates that the temporal signal's strength obtained with the EOF method's application highly depends on the noise level. In particular, the noise in the data can substantially reduce the first EOFs percentage of variability, even for clearly visible and defined spatial patterns. For example, in Fig. 3 (d, e) and Fig. 4 (d, e) the observed patterns are quite prominent, but the percentage of the recovered variability is less than 30% and 40% for zonal and meridional patterns, respectively. This

indicates that even when the retrieved percentage of variability by the EOF method is relatively low, the method can detect correct patterns.

Considering that no other pattern was introduced in the simulated data, all the retrieved temporal variabilities by the 2nd and 3rd EOFs modes should be not real and caused by fake patterns picked up in the random noise. The second and third EOF modes for both scenarios retrieve less than 10% of the variance. This percentage then can be used as an indication of the reliability of the EOF method. Therefore, any EOF mode with a percentage of less than 10% variability is caused purely by noise and is unreliable.

To test whether there is any preference in detecting the meridional pattern better than the zonal one, the variance retrieved by the EOF method for both scenarios was compared. The difference of retrieved variance for scenarios A and B varies between 10% and 21% (Fig. 5). At low noise levels, the difference is marginal (10%). It increases with the introduced uncertainty until the noise level reaches 20% when the difference starts to decrease. Overall, the method exhibited a slight preference for detecting the meridional pattern compared to the zonal one. This feature reflects a higher density of satellite measurements in the east-west direction at the Baltic Sea latitudes.

3. Results

3.1 Spatial distribution of wave heights

The first EOF mode of the Baltic Sea wave heights over the whole period (Fig. 6a) shows high values in the Baltic proper, both in the southern and eastern parts. The lower values are observed in the Gulf of Finland, the Gulf of Riga, the Danish straits, and the Gulf of Bothnia. This spatial pattern in the central Baltic Sea qualitatively matches the results of the EOF analysis of the modelled wave climate (Mietus and von Storch 1997), where the first EOF mode also showed higher values in the eastern part of the Baltic proper.

To study the seasonality of wave patterns, two approaches are used. The first one uses the classification of the seasons into "stormy" period, which includes the months from January to March and from August to December and the "calm" period, which lasts from April to July (Soomere and Pindsoo 2016; Männikus et al. 2020). The EOFs are also considered for regular seasons, such as winter (DJF, Fig. 7a), spring (MAM, Fig. 6b), summer (JJA, Fig. 6c), and fall (SON, Fig. 6d). The spring and fall seasons reveal a north-south structure, the spring showing higher values of the first EOF in the northern parts of the Baltic Sea, in the Bay of Bothnia (Fig. 6b), whereas the fall exhibit an EOF structure with the maxima in the southern Baltic and the Baltic proper (Fig. 6d). The EOFs for the summer season (Fig. 6c) revealed strong patchiness without a prominent large-scale pattern. The fall and spring have the most and the least number of satellite altimetry snapshots, respectively (Fig. 8). The percentages of retrieved variance with the EOF analysis are shown for different seasons and the whole year in Table 1. The total temporal variability, explained by the first three EOF functions, ranges from 38% for the calm period up to 44% in winter.

Seasons	First EOF (%)	Second EOF (%)	Third EOF (%)	Total variability (%)
Winter	27	9	8	44
Spring	17	14	12	43
Summer	22	9	8	39
Fall	23	9	7	39
Stormy	19	12	8	39
Calm	17	11	10	38
All seasons	17	13	10	40

Table 1 Temporal variability explained by EOF modes during different seasons.

The winter season showed the strongest signal in the first EOF. Additionally, this season revealed a prominent meridional pattern (Fig. 7a). The first EOF mode is negative in the eastern part of the Baltic proper and the eastern part of the Gulf of Bothnia, whereas it shows positive values in the western parts of these water bodies. The meridional pattern is remarkably similar to the spatial distribution of linear trends (Fig. 7b) fitted to the winter season yearly averages for 1996–2015 period (the detailed description of trends is discussed in Kudryavtseva and Soomere 2017).

The linear trends are shown in Fig. 7b are fitted using the same grid like the one used for the EOF analysis (Section 2.2) for better comparability of the results. However, instead of the monthly averaging, the seasonal averaging was performed. The trends were fitted for each grid cell, and only the trends with the statistical significance >95% are shown in Fig. 7b. The probability of the coincidence that statistically significant linear trends are detected in the same cell as the first EOF with the values higher than a particular cut-off value was thoroughly tested. The selection of values above the cut-off value of –0.07 provided the highest probability of coincidence. This cut-off value results in 77% of grid cells with the detected linear trends coinciding with the first winter EOF pattern. This means that 77% of grid cells with the significant linear trend are located precisely at the same locations as the grid cells with winter EOF above –0.07. Therefore, the statistically significant trends' location is remarkably similar to the first EOF function, meaning *that the first winter EOF is associated with the linear trends in SWH*.

3.2 Reliability of spatial patterns

In this study, the variance explained by the first EOF is only ~27% for the winter season. The model-based studies of wave climate with the EOF method revealed a much stronger signal in the Baltic Sea (Mietus and von Storch 1997; Shimura, Mori and Mase 2013). However, similar satellite-based studies also reported a low percentage of the retrieved variance of the first EOF. For example, Hemer, Church and

Hunter (2010) using multi-mission altimeter data, found that the first EOFs of the wave climate explain only 17–19% of the wave climate variability. Similarly, Woolf, Challenor and Cotton (2002) found that for the North Atlantic satellite-derived wave climate the first EOF explains 41% of the variance, while the other EOFs explain <19% of temporal variability each. The retrieved variance's dependence on the gaps and noise in the satellite altimetry data are not widely discussed.

The detailed analysis of the simulated datasets performed in Section 2.4 demonstrates that the noise level in the satellite data significantly affects the percentage of retrieved variance and that the shape of the retrieved spatial patterns is practically not affected (Fig. 5). With the considerable noise level, the amount of temporal variability explained by the first EOF can become as low as 20% even for a very distinctive and robust pattern in simulated data. However, even with high noise levels and the low percentage of variability, the EOF method can still reconstruct the correct spatial pattern (Fig. 3e, Fig. 4e). Therefore, the lower variance retrieved with the EOF method from satellite altimetry data (e.g., Hemer, Church and Hunter 2010) is most likely caused by the data's substantial uncertainty. Hence, it is likely that the observed meridional pattern in the first EOF (Fig. 7a) does represent a real pattern of the wave climate, even if it has a relatively low percentage of retrieved variance.

3.3 Relation between SWH trends and large-scale atmospheric teleconnections

To study whether the Baltic Sea wave climate and trends in wave height are driven by the changes in the large-scale atmospheric circulation, a correlation analysis was performed between the first three EOFs, signifying the spatio-temporal modes of the Baltic Sea wave climate, and various climatic indices. To match the satellite altimetry data's monthly timescales, the monthly time series of the climatic indices were used. The climatic records were obtained from the NOAA Center for Weather and Climate Prediction.

The strongest correlation between the first EOF for the winter season and the Scandinavia (SCAND) climatic index is negative, with a correlation coefficient of –0.47±0.19 (Table 2). The SCAND mode exhibits substantial seasonal variability. Interestingly, the correlation of the first EOF mode with the SCAND also shows variability over different seasons. It is the lowest throughout the spring season (0.24±0.22). During the summer and fall it is positive, 0.38±0.20 and 0.36±0.21 respectively, reflecting a prevailing (south-)easterly wind direction during these seasons.

The uncertainty of the correlation, evaluated in terms of the 95% confidence intervals, was used as a measure of reliability. Only three studied climatic indices exhibit a correlation larger than the uncertainty intervals for the winter season, namely the SCAND, the AO, and the NAO indices. Contrary to the SCAND index, the AO and NAO show positive correlations, with the coefficients of 0.42±0.20 (AO) and 0.31±0.22 (NAO). Both the AO and NAO have a significant correlation with the first EOF mode during the winter season. For all other seasons, this mode reveals no correlations larger than uncertainty. The correlation analysis performed between the other climatic indices, namely AMO, EA, EAWR, POLEUR and the first three EOFs resulted in no significant correlation. The EAWR index showed a correlation coefficient of 0.26±0.22 with the first winter EOF, which is slightly higher than the associated uncertainty.

The estimated values of correlation coefficients are close to similar values from correlation analysis between the annual number of storms in the Baltic Sea with the wave heights larger than 2 m and various teleconnections reported by Myslenkov et al. (2018) and Medvedeva et al. (2016) where they found a correlation of –0.59 with the SCAND, 0.32 with the AO, and 0.12 with the NAO index based on the wave modelling results and NCAR reanalysis. The similarity of the found correlation coefficients indicates that the first winter EOF and the wave heights trends are affected by the same processes as the storminess. Slightly stronger positive correlations with the NAO and AO indices and a weaker negative correlation with the SCAND index were obtained for significant wave heights (SWH) >4 m using wave hindcast for a more extended period of 1950–2010 (Surkova, Arkhipkin and Kislov 2015). A stronger positive correlation is most likely caused by the rapid reaction of wave fields to the time variability of the main teleconnection patterns' influence over the Baltic Sea region.

The relationship between the wave height variability and the climatic indices was also studied at a few wave measurement locations. Wave records at Vilsandi at the West Estonian Archipelago showed a correlation of the SWH with the NAO indices at the level of 0.7 during 1966–2006 (Suursaar and Kullas 2009). However, only a mild relation between the NAO index and wave heights was found in the southern Baltic (e.g., at Lubiatowo in January (Różyński 2010)). Therefore, it is likely that the impact of phenomena that govern the NAO index on the Baltic Sea wave fields dramatically varies in different locations and periods. This feature is not unexpected because the Baltic Sea wave climate's severity substantially depends on the match of predominant strong wind directions with this water body's geometry.

Climatic Index	First EOF	Second EOF	Third EOF
SCAND	–0.47±0.19	0.01±0.24	–0.07±0.24
AO	0.42±0.20	0.19±0.23	–0.03±0.24
NAO	0.31±0.22	0.19±0.23	–0.09±0.24

Table 2 Correlation coefficients between climatic indices and first three EOFs for the winter season.

3.4 Time variable correlation with climatic indices

To study possible time variability of the influence of the climatic indices on the wave climate of the Baltic Sea, a sliding correlation analysis is performed. A Pearson's product-moment correlation implemented in the "stats" package (R version 3.4.4) is used for the correlation analysis between the first three dominant climatic indices (SCAND, AO, and NAO) during the winter months and the first EOF in winter. Kendall and Spearman's correlations are also calculated and lead to the same results. Different window sizes from 2 to 9 years are tested (with one-year step), and the window with a length of 5 years is selected as it provides the optimal noise level.

For all three studied climatic indices, the sliding correlation coefficients (called correlations below for brevity) with the first winter EOF exhibit significant time variability (Fig. 9). The SCAND index revealed the

highest values (between −0.5 and −0.8) from 2000 to 2009. The correlation with the SCAND index was statistically significant at a >95% level during these years. The significance is calculated in a classical manner using the Pearson *p*-value criteria of <0.05, which considers both the magnitude of correlation and the number of entries in the time series. The SCAND index has a predominantly negative correlation with the first winter EOF mode. After 2009 the interrelation of the index and the wave climate in the Baltic Sea drastically diminishes.

The sliding correlation between the AO index and the first EOF is in the range of 0.16–0.66, reaching the maximum in 2012. Throughout 2008–2012, the correlation had a robust value of ~0.55 and was statistically significant at a 95% level. The maximum correlation for the NAO index was 0.72 in 2010. Between 2009 and 2012, the correlation surged and had the most reliable values (above >0.5) and was consistently statistically significant at a 95% level. The correlation with the AO and NAO indices gradually increased from 2008 until 2012. The NAO index surged to the highest value in 2009 and fluctuated until 2012, while the AO index increased more slowly than the NAO index over this period.

Our analysis shows that the NAO and AO indices' correlation with the winter first EOF was rather low in 1995–2009. A significant change occurred after 2009 when the SCAND index's effect diminishes, and the NAO and AO indices exhibit a strong correlation with the winter wave climate. Similarly to other studies, the AO and NAO indices show related behaviour. Among these climatic indices, the SCAND index had a stronger correlation with the winter wave climate between 2000 and 2009, and after this year, its effect reduced. The years 2008–2009 represent a turning moment in the Baltic Sea wave climate when the correlation with the SCAND index drastically diminished, and, at the same time, the correlation with the NAO and AO indices became statistically significant at a >95% significance level and stayed at the same level after 2009.

4. Discussion And Conclusions

In order to interpret the appearance of various modes and parameters of the EOF modes of the Baltic Sea wave climate derived from satellite altimetry, it was demonstrated that (i) the percentage of variability in the retrieved wave fields is directly related to the percentage of noise in the data and that (ii) the retrieved spatial patterns are practically not affected by the noise. Low variance is generally observed in the EOF analysis of the wave climate derived from the satellite altimetry (e.g., Woolf, Challenor and Cotton, 2002; Hemer, Church and Hunter 2010). However, the reasons behind the low retrieved variance of EOFs were not studied in detail. In this study, a thorough analysis was performed on how the measurements' noise affects the retrieve variance of EOF modes.

The connection between the NAO index and trends in the wave heights for the North Atlantic and the North Sea is well-established and widely discussed (e.g., Woolf, Challenor and Cotton 2002; Wolf and Woolf 2006; Hemer, Church and Hunter 2010). The phenomena behind the NAO index are driving processes in those bodies of water. For example, the long-term positive trend in the wave heights in the North Atlantic (Bertin, Prouteau and Letetrel 2013) is related to the corresponding trend in the NAO index

(e.g., Wolf and Woolf 2006). However, it was not clear if there is a connection between the wave climate trends and climatic indices in the Baltic Sea region. The results of our study show a strong anti-correlation between the linear trends in the Baltic Sea wave climate and the SCAND climatic index (–0.47±0.19) and a positive correlation with the NAO (0.31±0.22) and AO (0.42±0.20) indices. During the NAO and AO's positive phase, strong westerly winds predominate in the Baltic Sea area (Fig. 7b). This negative correlation with the SCAND index and a positive correlation with the NAO and AO indices agrees well with the explanation that the trends in the Baltic Sea wave climate are due to the interplay of north-westerly (driven by the SCAND teleconnection) and westerly (driven by the NAO and AO) winds over the region.

Most importantly, using the running correlation analysis, we demonstrated for the first time that the Baltic Sea wave climate has a significant time variable correlation with the SCAND, NAO, and AO indices. The phenomena that govern the SCAND mode had a strong influence on the Baltic Sea waves between 2000 and 2009 when the effect of the NAO and AO indices was weak. Interestingly, after the year 2009, the correlation of wave properties with the SCAND index significantly diminished, and the NAO and AO indices exhibit a strong correlation with the winter wave climate. This feature can be interpreted as an indication that the Baltic Sea wave climate is driven alternately by several sets of processes that are characterised by the listed three indices. The correlation of wave properties and a single index dramatically varies in time. When north-westerly winds are stronger during the negative phase of the SCAND index, the effect of the processes that drive the NAO index is weaker. Alternatively, when the correlation with the NAO index is more substantial, the westerly winds are stronger, and the effect of phenomena that make up the SCAND index is weaker.

Declarations

Funding. The research was co-supported by the institutional financing by the Estonian Ministry of Education and Research (grant IUT33-3), the Flag-ERA project FuturICT2.0.

Availability of data and material. The RADS satellite altimetry data are available at http://rads.tudelft.nl/rads/rads.shtml.

Code availability. From the authors on request.

Competing interests: The authors declare that they have no conflict of interest.

Acknowledgement

The research was co-supported by the institutional financing by the Estonian Ministry of Education and Research (grant IUT33-3), the Flag-ERA project FuturICT2.0 and the Estonian Research Council (grant PRG1129). We also acknowledge the support of the Horizon2020 Erasmus+ project CUPAGIS in terms of institutional collaboration. We thank the Radar Altimeter Database System (RADS) database and NOAA

Center for Weather and Climate Prediction for providing the data. Comments on the manuscript from anonymous referees are greatly acknowledged.

References

Andersson HC (2002) Influence of long-term regional and large-scale atmospheric calculation on the Baltic sea level. Tellus A: Dynamic Meteorology and Oceanography 54(1):76–88.

Barbariol F, Bidlot J-R, Cavaleri L, Sclavo M, Thomson J, Benetazzo A (2019) Maximum wave heights from global model reanalysis. Progress in Oceanography 175:139–160. https://doi.org/10.1016/j.pocean.2019.03.009

Barnston AG, Livezey RE (1987) Classification, seasonality and persistence of low-frequency atmospheric circulation patterns. Monthly Weather Review 115(6):1083–1126, https://doi.org/10.1175/1520-0493(1987)115<1083:CSAPOL>2.0.CO;2

Bednorz E, Czernecki B, Tomczyk AM, Półrolniczak M (2018) If not NAO then what?—regional circulation patterns governing summer air temperatures in Poland. Theoretical and Applied Climatology 136: 1325–1337.

Bertin X, Prouteau E, Letetrel C (2013) A significant increase in wave height in the North Atlantic Ocean over the 20th century. Global and Planetary Change 106:77–83. https://doi.org/10.1016/j.gloplacha.2013.03.009

Booij N, Ris RC, Holthuijsen LH (1999) A third-generation wave model for coastal regions: 1. Model description and validation. Journal of Geophysical Research–Oceans 104(C4):98JC02622: 7649–7666. https://doi.org/10.1029/98JC02622

Björkqvist J-V, Lukas I, Alari V, van Vledder GP, Hulst S, Pettersson H, Behrens A, Männik A (2018) Comparing a 41-year model hindcast with decades of wave measurements from the Baltic Sea. Ocean Engineering 152:57–71. https://doi.org/10.1016/j.oceaneng.2018.01.048

Björkqvist J-V, Rikka S, Alari V, Männik A, Tuomi L, Pettersson H (2020) Wave height return periods from combined measurement-model data: a Baltic Sea case study. Natural Hazards and Earth System Sciences, 20(12):3593–3609. https://doi.org/10.5194/nhess-20-3593-2020

Brenner AC, Bindschadler RA, Thomas RH, Zwally HJ (1983) Slope-induced errors in radar altimetry over continental ice sheets. Journal of Geophysical Research 88(C3):1617–1623. https://doi.org/10.1029/JC088iC03p01617

Bueh C, Nakamura H (2007) Scandinavian pattern and its climatic impact. Quarterly Journal of the Royal Meteorological Society 133(629):2117–2131. https://doi.org/10.1002/qj.173

Cañellas B, Orfila A, Méndez F, Álvarez A, Tintoré J (2010) Influence of the NAO on the northwestern Mediterranean wave climate. Scientia Marina 74(1):55–64 https://doi.org/10.3989/scimar.2010.74n1055

Church JA, White NJ, Coleman R, Lambeck K, Mitrovica JX (2004) Estimates of the regional distribution of sea level rise over the 1950–2000 period. Journal of Climate 17(13):2609–2625. https://doi.org/10.1175/1520-0442(2004)017<2609:EOTRDO>2.0.CO;2

Cieślikiewicz W, Paplińska-Swerpel, B (2008) A 44-year hindcast of wind wave fields over the Baltic Sea. Coastal Engineering 55(11):894–905. https://doi.org/10.1016/j.coastaleng.2008.02.017

Gao T, Yu J-Y, Paek H (2017) Impacts of four northern-hemisphere teleconnection patterns on atmospheric circulations over Eurasia and the Pacific. Theoretical and Applied Climatology, 129(3–4):815–831. https://doi.org/10.1007/s00704-016-1801-2

Hannachi A (2004) A Primer for EOF Analysis of Climate Data. Department of Meteorology, University of Reading: Reading, UK. http://www.o3d.org/eas-6490/lectures/EOFs/eofprimer.pdf.

Hasselmann K, Hasselmann S, Bauer E, Janssen P, Komen GJ, Bertotti L, Lionello P (1988) The WAM Model—A third generation ocean wave prediction model. Journal of Physical Oceanography 18 (12):1775–1810. https://doi.org/10.1175/1520-0485(1988)018<1775:TWMTGO>2.0.CO;2

Hemer MA, Church JA, Hunter JR (2010) Variability and trends in the directional wave climate of the Southern Hemisphere. International Journal of Climatology 30(4):475–491. https://doi.org/10.1002/joc.1900

Hemer MA, Fan Y, Mori N, Semedo A, Wang XL (2013) Projected changes in wave climate from a multi-model ensemble. Nature Climate Change 3(5):471–476. https://doi.org/10.1038/nclimate1791

Irannezhad M, Marttila H, and Kløve B (2014) Long-term variations and trends in precipitation in Finland. International Journal of Climatology 34(10):3139–3153. https://doi.org/10.1002/joc.3902

Izaguirre C, Méndez JF, Menéndez M, Losada IJ (2011) Global extreme wave height variability based on satellite data. Geophysical Research Letters 38(10):L10607. https://doi.org/10.1029/2011GL047302

Jaagus J (2009) Regionalisation of the precipitation pattern in the Baltic Sea drainage basin and its dependence on large-scale atmospheric circulation. Boreal Environment Research 14: 31–44.

Jacobeit J, Jönsson P, Bärring L, Beck C, Ekström M (2001) Zonal indices for Europe 1780–1995 and running correlations with temperature. Climatic Change 48(1):219–241. https://doi.org/10.1023/A:1005619023045

Jevrejeva S, Moore JC, Grinsted A (2003) Influence of the Arctic Oscillation and El Niño-Southern Oscillation (ENSO) on ice conditions in the Baltic Sea: The wavelet approach. Journal of Geophysical Research D: Atmospheres 108(21):ACL10-1–ACL10-11.

Jevrejeva S, Moore JC, Woodworth PL, Grinsted A (2005) Influence of large-scale atmospheric circulation on European sea level: Results based on the wavelet transform method. Tellus, Series A: Dynamic Meteorology and Oceanography 57(2):183–193. https://doi.org/10.1111/j.1600-0870.2005.00090.x

Jönsson A, Broman B, Rahm L (2002) Variations in the Baltic Sea wave fields. Ocean Engineering 30(1):107–126. https://doi.org/10.1016/S0029-8018(01)00103-2

Kelpšaite L, Herrmann H, Soomere T (2008) Wave regime differences along the eastern coast of the Baltic Proper. Proceedings of the Estonian Academy of Sciences 57(4):225–231. https://doi.org/10.3176/proc.2008.4.04

Komen GJ, Cavaleri L, Donelan M, Hasselmann K, Hasselmann S, Janssen PAEM (1997) Dynamics and Modelling of Ocean Waves. Cambridge: Cambridge University Press.

Kudryavtseva NA, Soomere T (2016) Validation of the multi-mission altimeter wave height data for the Baltic Sea region. Estonian Journal of Earth Sciences 65(3):161–175. https://doi.org/10.3176/earth.2016.13

Kudryavtseva N, Soomere T (2017) Satellite altimetry reveals spatial patterns of variations in the Baltic Sea wave climate. Earth System Dynamics 8(3):697–706. https://doi.org/10.5194/esd-8-697-2017

Lionello P, Sanna A (2005) Mediterranean wave climate variability and its links with NAO and Indian Monsoon. Climate Dynamics 25(6):611–623. https://doi.org/10.1007/s00382-005-0025-4

Madsen KS, Høyer JL, Tscherning CC (2007) Near-coastal satellite altimetry: Sea surface height variability in the North Sea-Baltic Sea area. Geophysical Research Letters 34(14):L14601. https://doi.org/10.1029/2007GL029965

Männikus R, Soomere T, Viška M (2020) Variations in the mean, seasonal and extreme water level on the Latvian coast, the eastern Baltic Sea, during 1961–2018. Estuarine, Coastal and Shelf Science, 245:106827. https://doi.org/10.1016/j. ecss.2020.106827

Masselink G, Castelle B, Scott T, Dodet G, Suanez S, Jackson D, Floc'h F (2016) Extreme wave activity during 2013/2014 winter and morphological impacts along the Atlantic coast of Europe. Geophysical Research Letters 43(5):2135–2143. https://doi.org/10.1002/2015GL067492

Medvedeva A, Myslenkov S, Medvedev I, Arkhipkin V, Krechik V, Dobrolyubov S (2016) Numerical modeling of the wind waves in the Baltic Sea using the rectangular and unstructured grids and the reanalysis NCEP/CFSR. Proceedings of the Hydrometeorological Research Center of the Russian Federation (362):37–54 (in Russian with English summary).

Mietus M, von Storch H (1997) Reconstruction of the Wave Climate in the Proper Baltic Basin, April 1947–March 1988. GKSS Report 97/E/28, Geesthacht.

Myslenkov SA, Medvedeva A, Arkhipkin V, Markina M, Surkova G, Krylov A, Dobrolyubov S, Zilitinkevich S, Koltermann P (2018) Long-term statistics of storms in the Baltic, Barents and White seas and their future climate projections. Geography, Environment, Sustainability 11(1):93–112. https://doi.org/10.24057/2071-9388-2018-11-1-93-112

Nezlin NP, McWilliams JC (2003) Satellite data, Empirical Orthogonal Functions, and the 1997–1998 El Nino off California. Remote Sensing of Environment 84(2):234–254. https://doi.org/10.1016/S0034-4257(02)00109-8

Nikolkina I, Soomere T and Räämet A (2014) Multidecadal ensemble hindcast of wave fields in the Baltic Sea. The 6th IEEE/OES Baltic Symposium Measuring and Modeling of Multi-Scale Interactions in the Marine Environment, May 26–29, Tallinn Estonia. IEEE Conference Publications 6887854. https://doi.org/10.1109/BALTIC.2014.6887854

Niroomandi A, Ma G, Ye X, Lou S, Xue P (2018) Extreme value analysis of wave climate in Chesapeake Bay. Ocean Engineering 159:22–36. https://doi.org/10.1016/j.oceaneng.2018.03.094

Omstedt A, Pettersen C, Rodhe J, Winsor P (2004) Baltic Sea climate: 200 yr of data on air temperature, sea level variation, ice cover, and atmospheric circulation. Climate Research 25(3):205–216. https://doi.org/10.3354/cr025205

Patra A, Bhaskaran PK (2016) Trends in wind-wave climate over the head Bay of Bengal region. International Journal of Climatology 36(13):4222–4240. https://doi.org/10.1002/joc.4627

Passaro M, Cipollini P, Benveniste J (2015) Annual sea level variability of the coastal ocean: The Baltic Sea-North Sea transition zone. Journal of Geophysical Research-Oceans 120(4):3061–3078. https://doi.org/10.1002/2014JC010510

Räämet A, Soomere T, Zaitseva-Pärnaste I (2010) Variations in extreme wave heights and wave directions in the north-eastern Baltic Sea. Proceedings of the Estonian Academy of Sciences 59(2):182–192. https://doi.org/10.3176/proc.2010.2.18

Rikka S, Pleskachevsky A, Uiboupin R, Jacobsen S (2018) Sea state in the Baltic Sea from space-borne high-resolution synthetic aperture radar imagery. International Journal of Remote Sensing 39(4):1256–1284. https://doi.org/10.1080/01431161.2017.1399475

Różyński G (2010) Long-term evolution of Baltic Sea wave climate near a coastal segment in Poland; its drivers and impacts. Ocean Engineering 37(2–3):186–199. https://doi.org/10.1016/j.oceaneng.2009.11.008

Sartini L, Besio G, Cassola F (2017) Spatio-temporal modelling of extreme wave heights in the Mediterranean Sea. Ocean Modelling 117:52–69. https://doi.org/10.1016/j.ocemod.2017.07.001

Scharroo R (2012) RADS version 3.1 User Manual and Format Specifications. Available at http://rads.tudelft.nl/rads/ radsmanual.pdf [viewed 6 March 2020].

Scharroo R, Leuliette EW, Lillibridge JL, Byrne D, Naeije MC, Mitchum GT (2013) RADS: Consistent multi-mission products in Proc Symp on 20 Years of Progress in Radar Altimetry, 20–28 September 2012, Venice, Eur. Space Agency Spec. Publ., ESA SP-710.

Shimura T, Mori N, Mase H (2013) Ocean waves and teleconnection patterns in the northern hemisphere. Journal of Climate 26(21):8654–8670. https://doi.org/10.1175/JCLI-D-12-00397.1

Soomere T (2005) Wind wave statistics in Tallinn Bay. Boreal Environment Research 10(2):103–118

Soomere T, Behrens A, Tuomi L, Nielsen JW (2008) Wave conditions in the Baltic Proper and in the Gulf of Finland during windstorm Gudrun. Natural Hazards and Earth System Science 8(1):37–46. https://doi.org/10.5194/nhess-8-37-2008

Soomere T, Bishop SR, Viška M, Räämet A (2015) An abrupt change in winds that may radically affect the coasts and deep sections of the Baltic Sea. Climate Research 62(2):163–171. https://doi.org/10.3354/cr01269

Soomere T, Pindsoo K (2016) Spatial variability in the trends in extreme storm surges and weekly-scale high water levels in the eastern Baltic Sea. Continental Shelf Research 115:53–64. https://doi.org/10.1016/j.csr.2015.12.016

Soomere T, Räämet A (2011) Long-term spatial variations in the Baltic Sea wave fields. Ocean Science 7(1):141–150. https://doi.org/10.5194/os-7-141-2011

Soomere T, Räämet A (2014) Decadal changes in the Baltic Sea wave heights. Journal of Marine Systems 129:86–95. https://doi.org/10.1016/j.jmarsys.2013.03.009

Surkova GV, Arkhipkin VS, Kislov AV (2015) Atmospheric circulation and storm events in the Baltic Sea. Open Geosciences 7(1):332–341. https://doi.org/10.1515/geo-2015-0030

Suursaar Ü, Kullas T (2009) Decadal variations in wave heights off Cape Kelba, Saaremaa Island, and their relationships with changes in wind climate. Oceanologia 51(1):39–61. https://doi.org/10.5697/oc.51-1.039

Suursaar Ü, Sooäär J (2007) Decadal variations in mean and extreme sea level values along the Estonian coast of the Baltic Sea. Tellus, Series A: Dynamic Meteorology and Oceanography 59(2):249–260. https://doi.org/10.1111/j.1600-0870.2006.00220.x

Thompson DWJ, Wallace JM (1998) The Arctic Oscillation signature in the wintertime geopotential height and temperature fields. Geophysical Research Letters 25(9):1297–1300. https://doi.org/10.1029/98GL00950

Trigo RM, Osborn TJ, Corte-Real JM (2002) The North Atlantic Oscillation influence on Europe: climate impacts and associated physical mechanisms. Climate Research 20(1):9–17. https://doi.org/10.3354/cr020009

Tuomi L, Kahma KK, Pettersson H (2011) Wave hindcast statistics in the seasonally ice-covered Baltic Sea. Boreal Environment Research 16(6):451–472.

Tuomi L, Kanarik H, Björkqvist J-V, Marjamaa R, Vainio J, Hordoir R, Höglund A, Kahma KK (2019) Impact of ice data quality and treatment on wave hindcast statistics in seasonally ice-covered seas. Frontiers in Earth Science 7:166. https://doi.org/10.3389/feart.2019.00166

Wakelin SL, Woodworth PL, Flather RA,Williams JA (2003) Sea-level dependence on the NAO over the NW European Continental Shelf. Geophys. Res. Lett. 30(7):1403, https://doi.org/10.1029/2003GL017041

Walker GT, Bliss EW (1932) World weather. V. Mem. R. Meteorol. Soc. 4:53–84.

Weisse R, von Storch H, Niemeyer HD, Knaack H (2012) Changing North Sea storm surge climate: An increasing hazard? Ocean & Coastal Management 68:58–68. https://doi.org/10.1016/j.ocecoaman.2011.09.005

Wolf J, Woolf DK (2006) Waves and climate change in the north-east Atlantic. Geophys Res Lett 33:L06604, https://doi.org/10.1029/2005GL025113

Woolf DK, Challenor PG, Cotton PD (2002) Variability and predictability of the North Atlantic wave climate. Journal of Geophysical Research C-Oceans, 107(C10):3145. https://doi.org/10.1029/2001JC001124

Figures

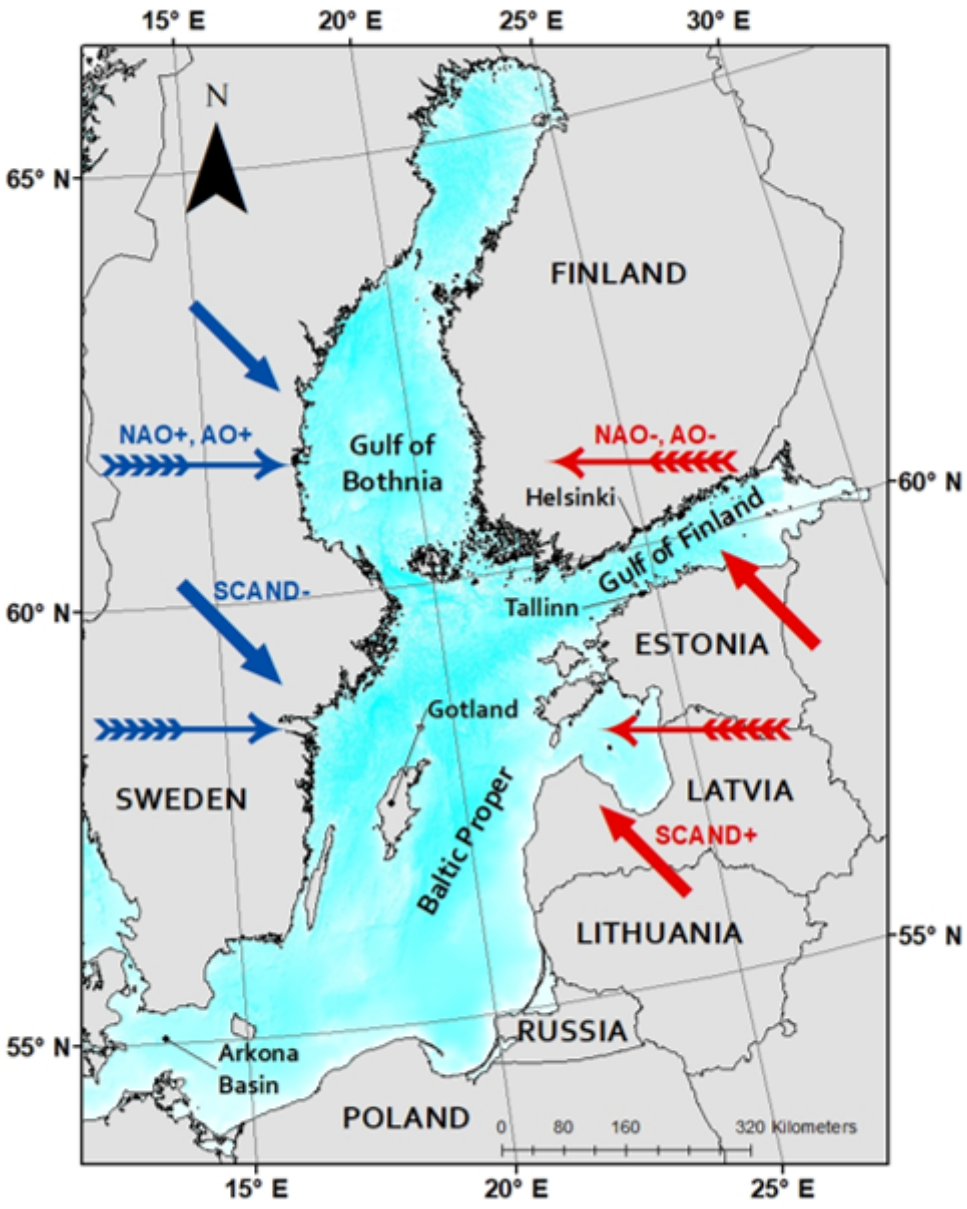

Figure 1

Map of the study area and the predominant wind direction during the positive (red) and negative (blue) phases of the SCAND, positive (blue) and negative (red) phases of NAO and AO patterns. Note: The designations employed and the presentation of the material on this map do not imply the expression of any opinion whatsoever on the part of Research Square concerning the legal status of any country, territory, city or area or of its authorities, or concerning the delimitation of its frontiers or boundaries. This map has been provided by the authors.

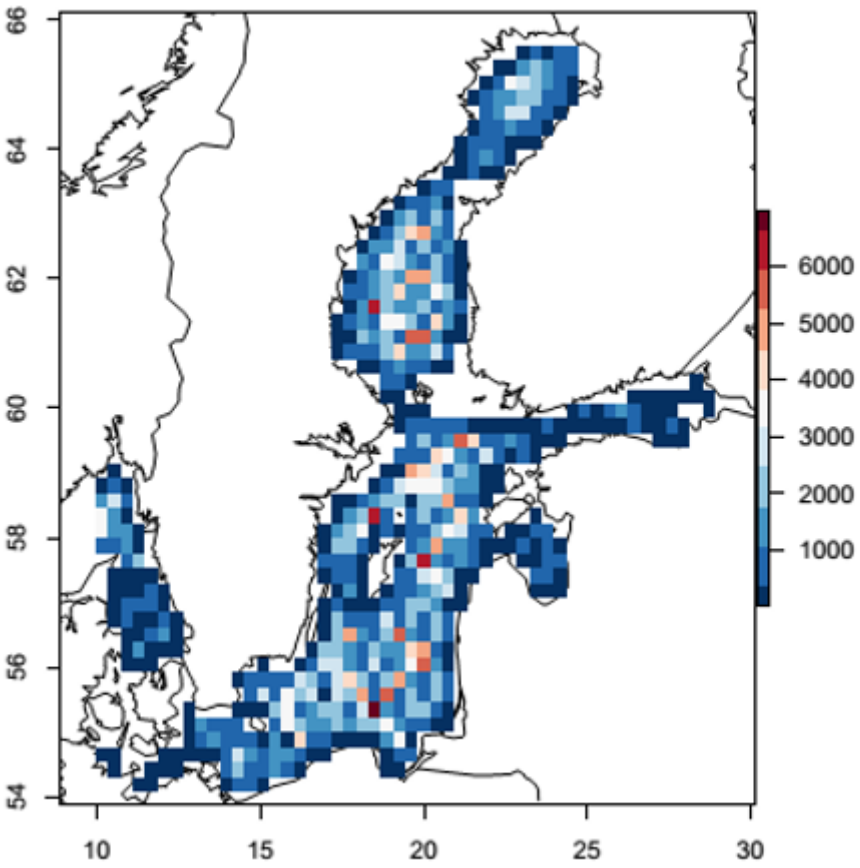

Figure 2

Spatial distribution of the number of satellite altimetry SWH data in the Baltic Sea for the period 1992–2015. Note: The designations employed and the presentation of the material on this map do not imply the expression of any opinion whatsoever on the part of Research Square concerning the legal status of any country, territory, city or area or of its authorities, or concerning the delimitation of its frontiers or boundaries. This map has been provided by the authors.

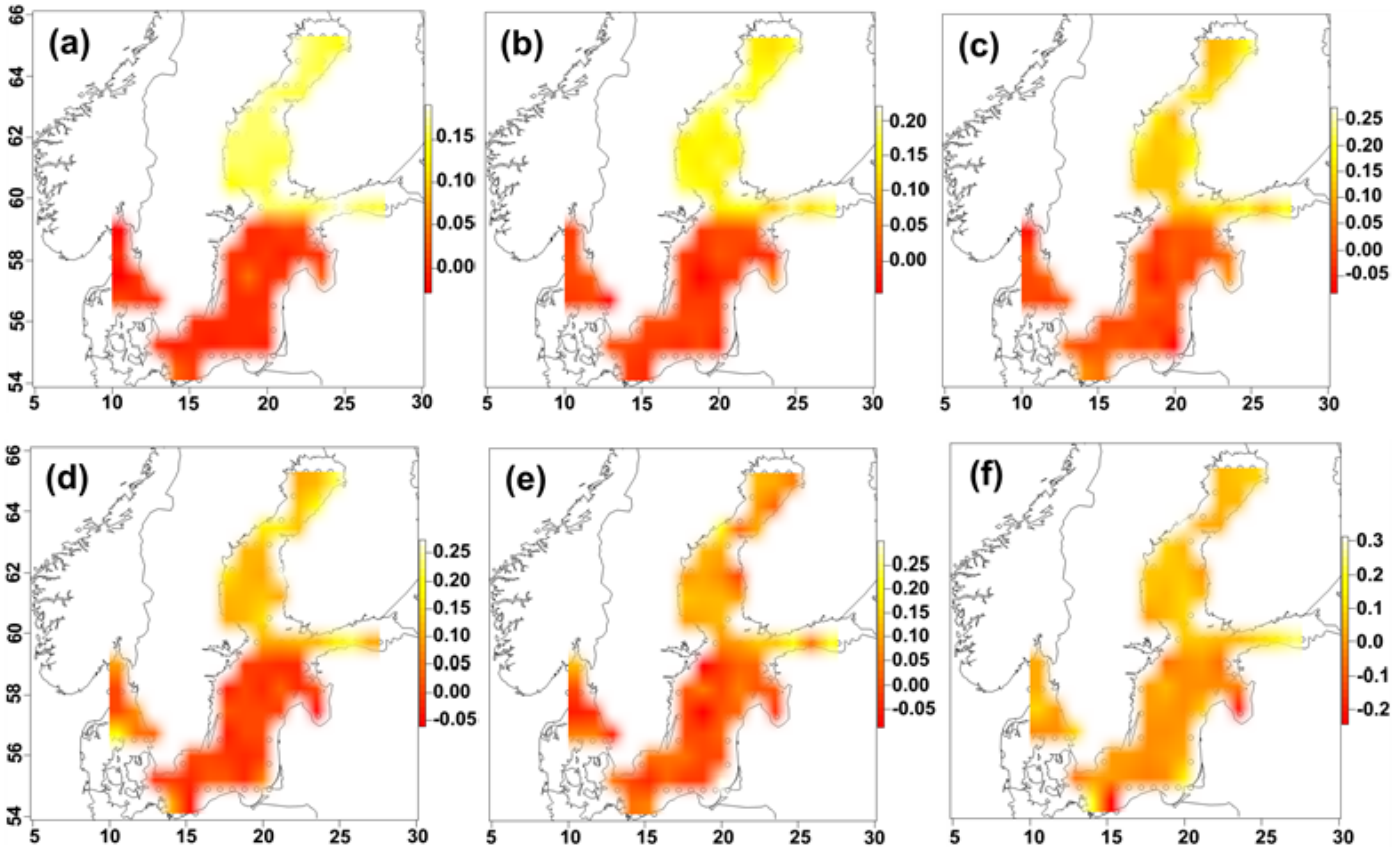

Figure 3

The first EOF patterns for simulated datasets (Scenario A) with introduced random noise at the level of 5% (a), 10% (b), 20% (c), 25% (d), 27% (e), and 30% (f). The figures were interpolated for ease of interpretation. Note: The designations employed and the presentation of the material on this map do not imply the expression of any opinion whatsoever on the part of Research Square concerning the legal status of any country, territory, city or area or of its authorities, or concerning the delimitation of its frontiers or boundaries. This map has been provided by the authors.

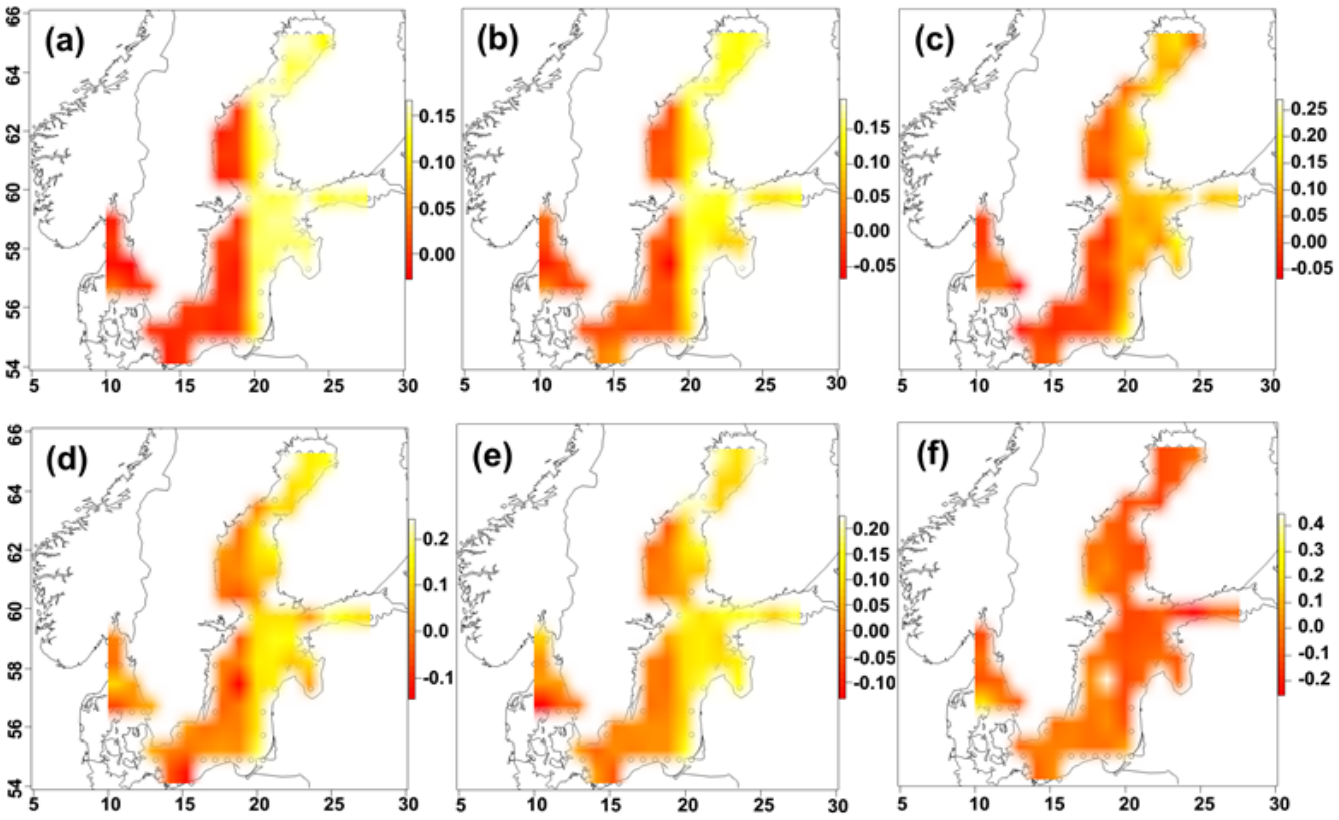

Figure 4

The first EOF patterns for simulated data (Scenario B) with introduced random noise at the level of 5% (a), 10% (b), 20% (c), 25% (d), 27% (e), and 30% (f). The figures were interpolated for ease of interpretation. Note: The designations employed and the presentation of the material on this map do not imply the expression of any opinion whatsoever on the part of Research Square concerning the legal status of any country, territory, city or area or of its authorities, or concerning the delimitation of its frontiers or boundaries. This map has been provided by the authors.

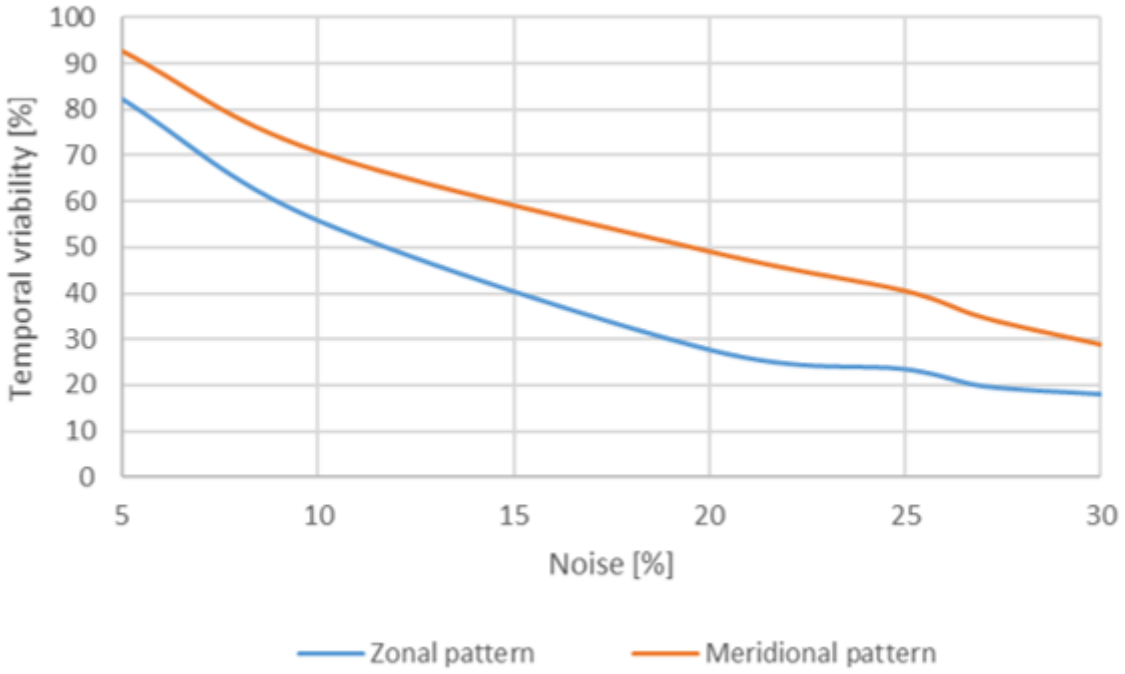

Figure 5

Reconstructed percentage of variability of the first EOF mode versus a percentage of introduced uncertainty in the synthetic datasets. The blue line represents the dataset with the introduced zonal pattern (Scenario A), and the orange line is the dataset with the meridional pattern (Scenario B).

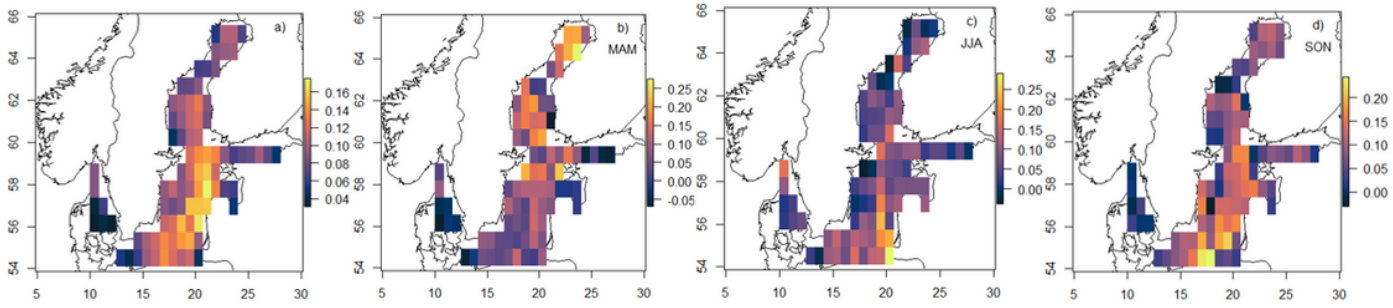

Figure 6

First EOFs describing the main patterns in the Baltic Sea wave heights retrieved for the entire SWH data set in (a), spring (b), summer (c), and fall (d) seasons. Note: The designations employed and the presentation of the material on this map do not imply the expression of any opinion whatsoever on the part of Research Square concerning the legal status of any country, territory, city or area or of its authorities, or concerning the delimitation of its frontiers or boundaries. This map has been provided by the authors.

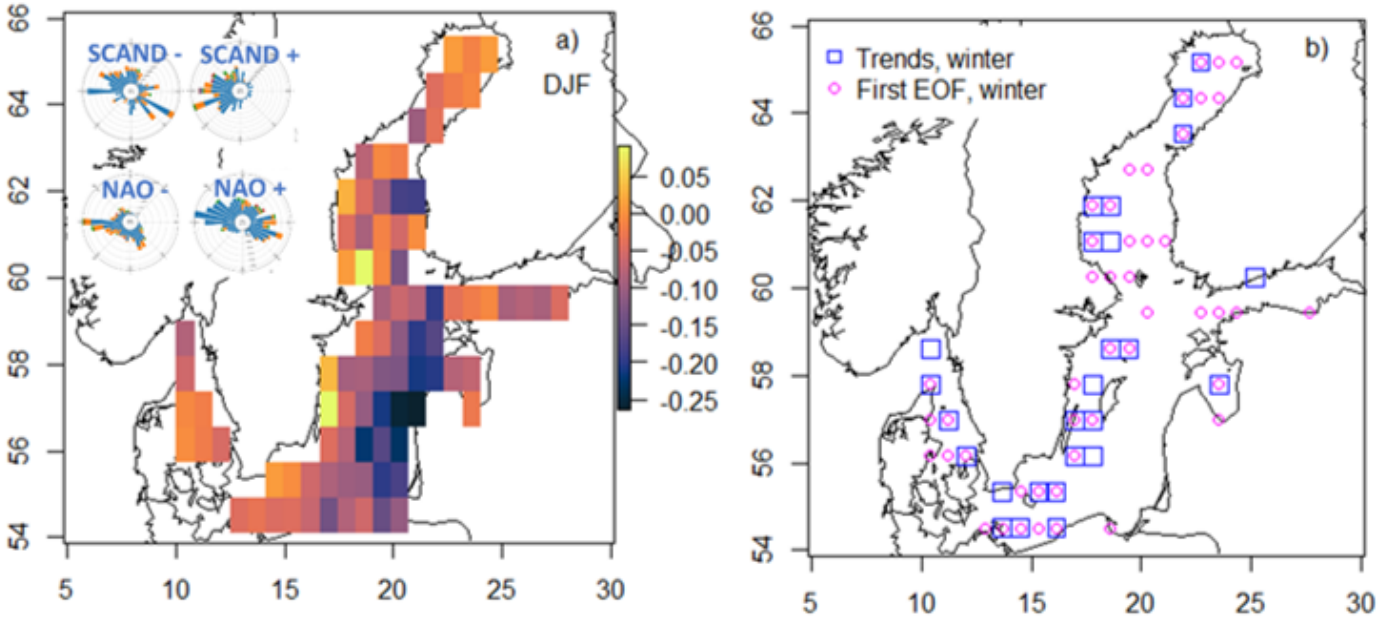

Figure 7

(a) The first EOF pattern for the winter season (DJF). The wind roses show typical winter wind direction during the SCAND positive (01 Dec 1998 – 26 Feb 1999) and negative (01 Dec 2005 – 28 Feb 2006) phases and the NAO positive (01 Dec 1994 – 28 Feb 1995) and negative (01 Dec 1995 – 28 Feb 1996) phases at Hultsfred station 57.53°N, 15.82°E (obtained from Swedish automatic wind measurement data, https://mesonet.agron.iastate.edu/sites/locate.php, last accessed 01 Feb 2021). (b) The spatial coincidence of the linear trends in SWH in winter and the first EOF mode in winter. The trends were fitted for 1996–2015 using the same grid like the one used for the EOF method and are significant at 95% confidence level. Only the EOF values above –0.07 are shown. Note: The designations employed and the presentation of the material on this map do not imply the expression of any opinion whatsoever on the part of Research Square concerning the legal status of any country, territory, city or area or of its authorities, or concerning the delimitation of its frontiers or boundaries. This map has been provided by the authors.

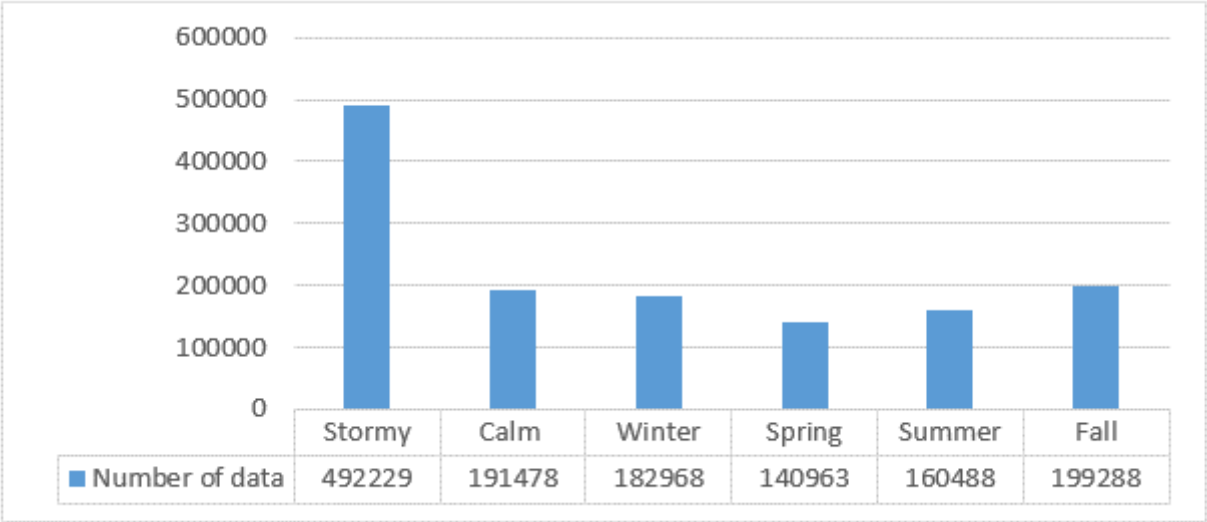

Figure 8

The total number of data in each season.

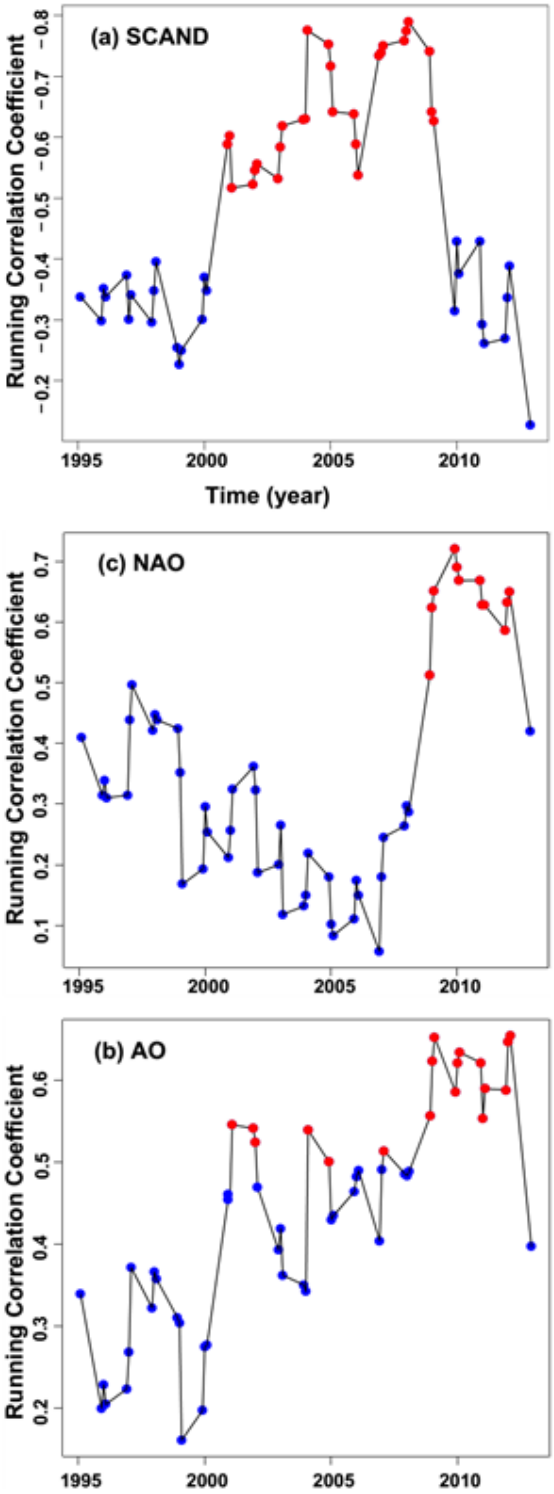

Figure 9

Sliding correlation coefficient between the first EOF and (a) Scandinavian mode, (b) Arctic Oscillation, and (c) the North Atlantic Oscillation with 5-year window size. The correlations with >95% level of statistical significance are indicated by red colour.